

**Decoherence effects on quantum control by reverse optimized pulse sequences**

C. A. Estrada Guerra, D. Velasco Villamizar, and Luis G. C. Rego

*Departamento de Física, Universidade Federal de Santa Catarina, Santa Catarina, CEP 88040-900, Brazil*

(Received 18 May 2012; published 17 August 2012)

The external coherent control over the dynamics of quantum systems has been the aim of many studies in recent years, and several theoretical frameworks have been devised for that purpose. However, several of the proposed methods have been developed to control isolated quantum systems, disregarding the decoherence effects that impinge on the ubiquitous open quantum systems that exhibit a more complex dynamics than their isolated counterparts. In this paper, we investigate the effects of dissipation and decoherence for a quantum-control procedure based on sequences of reverse optimized electromagnetic pulses. Although the method performs well for pure quantum systems, moderate decoherence and dissipation hinders its accomplishment for ordinary conditions, irrespective of the pulse sequence rate. The method can be appropriate, nonetheless, for dynamical decoupling of the quantum subsystem from the environment.

DOI: [10.1103/PhysRevA.86.023411](https://doi.org/10.1103/PhysRevA.86.023411)

PACS number(s): 32.80.Qk, 03.65.Yz, 34.10.+x, 02.60.Pn

**I. INTRODUCTION**

The goal of controlling quantum systems has been pursued by researchers of both scientific and technological realms [1]. The control over the coherent dynamics of quantum systems by means of externally applied electromagnetic pulses, in particular, has been the aim of many studies in recent years [2–8]. From the perspective of theory development, there are several coherent control schemes, including optimal control [9,10], coherent control over quantum trajectories [11], and closed-loop evolution [12,13], among others, which have been devised to guide experimental procedures for manipulating the coherent quantum dynamics [9,14,15]. Some of the proposed methods have been developed, however, upon the assumption that the quantum systems are isolated (closed) from their environment, since open quantum systems exhibit a much more complex dynamics than their isolated counterparts [16,17]. But oversimplified models may be unsuitable for describing a realistic physical situation, and that point is especially relevant for coherent control procedures, which should be tested against decoherence effects of the environment. The investigation of open quantum systems is, therefore, necessary for an accurate comprehension of the processes that occur in practical quantum-control implementations.

Decoherence is an ubiquitous phenomenon caused by the interaction of quantum systems with the environment, which induces the randomization of the quantum phases associated with a coherent superposition of states, making quantum-control techniques ineffective. For electronic excitations, the decoherence time scales range from femtoseconds to nanoseconds, mainly due to electron-electron and electron-phonon coupling mechanisms and spontaneous emission [18]. For spin-coherent states, decoherence takes place within microseconds to milliseconds, owing to coupling with other spins in the system and spin-orbit interaction [16]. Nevertheless, optical control procedures have been presented for the manipulation of physical observables in dissipative quantum systems, such as in the case of population transfer dynamics guided by laser pulses [19,20]. Other techniques have also been proposed to counteract the effects of environmentally driven decoherence in open quantum systems by manipulating

the coupling between system and environment [21]. Quantum error correction has been developed to cope with this challenge [22–24]. The closed-loop technique, in the form of fault-tolerant quantum error correction (QEC) [25,26], was the first to consider the problem of decoherence, whereas open-loop dynamical QEC was introduced as a promising alternative for dynamical decoupling (DD) [27–29]. If the parameters that characterize the environment are known, such as the effective coupling strength and the number of particles, then it is in principle possible to counteract its effects, but this is not always feasible.

This paper extends the theoretical framework of the quantum-control method based on reverse optimized pulse sequences [30] by taking into account an open quantum system in contact with a Markovian reservoir. The effectiveness of the procedure is analyzed for various situations and different degrees of decoherence and dissipation, wherein a quantum master equation is used to describe the dissipative coupling between a small quantum subsystem, comprised of a two-level system and an external electromagnetic field, and its environment. The control method is based on the reverse design framework for determining *a priori* the appropriate external field that takes the two-level system toward a desired quantum state. A sequence of reverse optimized electromagnetic pulses is utilized to control the dynamics of the expectation value for a quantum operator of the subsystem while, simultaneously, the purity of the quantum system is maintained at its highest value. The method is implemented by means of a nonlinear conjugate gradient method and it is applied to manipulate the population transfer dynamics within the two-level system. Although the procedure performs well for pure quantum systems, moderate decoherence hinders its effectiveness for ordinary dissipative conditions, irrespective of the applied pulse rate. The method is suited, nonetheless, for dynamical decoupling of the quantum subsystem from the environment.

The paper is organized as follows. Section II describes the master-equation approach and Sec. III develops the framework of the quantum-control method for an open quantum system. The results are presented and discussed in Sec. IV. The conclusions are presented in Sec. V.

## II. DYNAMICS OF AN OPEN QUANTUM SYSTEM

The Hamiltonian for the open quantum system can be written as

$$\mathbf{H} = \mathbf{H}_S + \mathbf{H}_E + \mathbf{H}_I, \quad (1)$$

where the terms of Eq. (1) denote the quantum subsystem of interest  $\mathbf{H}_S$ , the environment  $\mathbf{H}_E$ , and the interaction between the subsystem and its environment  $\mathbf{H}_I$ . The whole system follows the quantum dynamics governed by the Liouville equation ( $e = \hbar = 1$ )

$$i \frac{\partial}{\partial t} \rho(t) = [\mathbf{H}, \rho(t)], \quad (2)$$

where  $[\mathbf{H}, \rho(t)] \equiv \mathbf{H}\rho(t) - \rho(t)\mathbf{H}$ . By making use of the reduced density matrix  $\rho_S(t)$  that is obtained by taking the trace of the full density matrix over the environment degrees of freedom,  $\rho_S(t) = \text{Tr}_E\{\rho(t)\}$ , one gets the dynamical equation for the quantum subsystem  $S$ ,

$$\begin{aligned} i \frac{\partial}{\partial t} \rho_S(t) &= \text{Tr}_E\{[\mathbf{H}, \rho_S(t)]\} \\ &= [\mathbf{H}_S, \rho_S(t)] + \text{Tr}_E\{[\mathbf{H}_I, \rho(t)]\}, \end{aligned} \quad (3)$$

where we have used that  $\text{Tr}_E\{[\mathbf{H}_E(t), \rho(t)]\} = 0$  for the density matrix of the environment at  $t = 0$  represents a system in thermal equilibrium, which is diagonal in the energy eigenstate representation. Another, more convenient, way to write Eq. (3) is [31]

$$\frac{\partial}{\partial t} \rho_S(t) = -i[\mathbf{H}_S, \rho_S(t)] + \mathcal{L}\rho_S(t), \quad (4)$$

where the first term on the right-hand side describes the unitary part of the dynamical evolution of  $\rho_S(t)$  and the second term  $\mathcal{L}$  is the Liouville operator, also the denominated relaxation superoperator. The Liouville operator takes into account the nonunitary dynamics generated by the interaction of the subsystem with the environment. Within the physical conditions that satisfy the Born-Markov approximation [31], the temporal evolution of the reduced density matrix can be described by the quantum master equation in Lindblad form.

The validity of the Markovian approximation is determined by the characteristics of the environment vis-à-vis the system of interest and by their coupling [18,31,32]. By considering, for instance, an environment with an ohmic spectral density limited by the cutoff frequency  $w_c$ , the Markovian picture is valid for  $w_0 \ll w_c$ , where  $w_0$  is the characteristic frequency of the two-level system. Non-Markovian effects will start to arise for  $w_0 \approx w_c$ . Actually, a given system (a condensed-matter system, for example) can behave either way depending on the definition of the subsystem of interest and how it couples with the environment. In this paper, we chose to provide a general treatment for the effects produced by the environment, thus we adopt the Markovian approximation.

Let us assume that the open quantum system is constituted by a quantum subsystem, comprised of a two-level system interacting with a monochromatic classical electromagnetic field, and the environment that is represented by the vacuum state of the quantized electromagnetic field. In this case, the

master equation can be written, in the interaction picture, as

$$\begin{aligned} \frac{\partial}{\partial t} \rho_S &= -i[\mathbf{H}_S, \rho_S] + \mathcal{L}\rho_S \\ &= -i[\mathbf{H}_S, \rho_S] + \frac{1}{2}\Gamma(2\sigma_- \rho_S \sigma_+ - \sigma_+ \sigma_- \rho_S - \rho_S \sigma_+ \sigma_-), \end{aligned} \quad (5)$$

where  $\Gamma$  denotes the population decay rate from the excited state. Equation (5) takes into account the decoherence effects that result from the interaction between the subsystem and the environment. We assume that the spontaneous decay rate  $\Gamma$  is a constant and does not change due to the presence of the controlling electromagnetic pulse field [33]. The expectation value for any operator  $\mathbf{V}$  of the quantum subsystem is given by

$$\langle \mathbf{V}(t) \rangle = \text{Tr}\{\mathbf{V}\rho_S(t)\}. \quad (6)$$

Another quantity of relevance is the purity of the reduced density matrix,

$$\mathcal{P} \equiv \text{Tr}\{\rho_S^2(t)\}, \quad (7)$$

which provides a measure for the integrity of the quantum state describing the subsystem. The purity assumes values within the range  $1/d \leq \mathcal{P} \leq 1$ , with  $d$  being the dimension of the Hilbert space. The minimum value corresponds to a classical statistical mixture, whereas the maximum value stands for a pure quantum state represented by a ray in the underlying Hilbert space.

## III. CONTROL METHOD

The coherent control procedure is applied to an effective two-level system that is externally driven by a resonant monochromatic electromagnetic field. The coupling between the two-level system and the electromagnetic field is described by the dipole approximation, with the linearly polarized field written as  $E(t) = \mathcal{E}\exp(-i\omega t) + \text{c.c.}$ , where the field amplitude is a complex number  $\mathcal{E} = |\mathcal{E}|\exp(i\phi)$ . In the interaction picture, the Hamiltonian of the quantum subsystem (atomic and field systems) is written as

$$\mathbf{H}_S = -\Omega_R \begin{pmatrix} 0 & \exp(-i\varphi) \\ \exp(i\varphi) & 0 \end{pmatrix}, \quad (8)$$

in the basis of the ground  $|g\rangle$  and excited  $|e\rangle$  states, and  $\Omega_R = |\mathcal{E}||d|$  is the Rabi frequency. In Eq. (8),  $\langle n|\mathbf{H}_S|n\rangle = 0$  ( $n = g, e$ ) for the unperturbed states have well-defined parities, a typical case for dipolar interactions. In general, the transition dipole moment is also a complex number that is represented as  $d_{ge} = |d_{ge}|\exp(-i\theta)$ . Thus, without loss of generality, in Eq. (8) we defined the phase  $\varphi = \phi + \theta$  as the relative phase between the electromagnetic field and the dipole moment of the two-level system.

Substituting Eq. (8) into Eq. (5), we obtain a set of coupled differential equations for the matrix elements of  $\rho_S(t)$ ,

$$\frac{\partial}{\partial t} \rho_{gg} = i\Omega_R(\rho_{eg}e^{i\Delta t}e^{-i\varphi} - \rho_{ge}e^{-i\Delta t}e^{i\varphi}) + \Gamma\rho_{ee}, \quad (9a)$$

$$\frac{\partial}{\partial t} \rho_{ge} = i\Omega_R e^{i\Delta t} e^{-i\varphi} (\rho_{ee} - \rho_{gg}) - \gamma_{eg}\rho_{ge}, \quad (9b)$$

$$\frac{\partial}{\partial t} \rho_{eg} = i\Omega_R e^{-i\Delta t} e^{i\varphi} (\rho_{gg} - \rho_{ee}) - \gamma_{eg} \rho_{eg}, \quad (9c)$$

$$\frac{\partial}{\partial t} \rho_{ee} = i\Omega_R (\rho_{ge} e^{i\Delta t} e^{i\varphi} - \rho_{eg} e^{i\Delta t} e^{-i\varphi}) - \Gamma \rho_{ee}, \quad (9d)$$

where  $\Delta \equiv \omega - \omega_{eg}$  is the detuning and  $\gamma_{eg} = \Gamma/2$  is the relaxation rate of the quantum coherence. For memoryless Markovian systems, information on the properties of the

environment are in the form of decay rates. Generally, the decoherence relaxation rate can be written as  $\gamma_{eg} = \frac{1}{2}\Gamma + 2\Gamma_{\text{phase}}$ , where  $\frac{1}{2}\Gamma$  stands for the decoherence produced by interstate transitions (including spontaneous decay) and  $\Gamma_{\text{phase}}$  accounts for pure (elastic) decoherence mechanisms that do not affect the populations. Solving the differential equations for the resonant case,  $\Delta = 0$ , we find the time-dependent components of the reduced density matrix,

$$\begin{aligned} \rho_{gg}(t) = & -\frac{1}{\bar{\Omega}(\Gamma^2 + 8\Omega_R^2)} e^{-\frac{3}{4}\Gamma(t-t_0)} \left\{ -\sinh\left[\frac{\bar{\Omega}}{4}(t-t_0)\right] \{4i\Omega_R(\Gamma^2 + 8\Omega_R^2)[\rho_{eg}(t_0)e^{-i\varphi} - \rho_{ge}(t_0)e^{i\varphi}] \right. \\ & + \Gamma[12\rho_{gg}(t_0)\Omega_R^2 + \rho_{ee}(t_0)(20\Omega_R^2 + \Gamma^2)] \} + \cosh\left[\frac{\bar{\Omega}}{4}(t-t_0)\right] [-4\rho_{gg}(t_0)\Omega_R^2\bar{\Omega} + \rho_{ee}(t_0)\bar{\Omega}(\Gamma^2 + 4\Omega_R^2)] \\ & \left. - e^{\frac{3}{4}\Gamma(t-t_0)}\bar{\Omega}(\Gamma^2 + 4\Omega_R^2) \right\}, \end{aligned} \quad (10)$$

$$\begin{aligned} \rho_{ge}(t) = & -\frac{1}{2\bar{\Omega}(8\Omega_R^2 + \Gamma^2)} e^{-\frac{3}{4}\Gamma(t-t_0)} \left\{ \cosh\left[\frac{\bar{\Omega}}{4}(t-t_0)\right] \{ -\bar{\Omega}(8\Omega_R^2 + \Gamma^2)[\rho_{ge}(t_0) - e^{-2i\varphi}\rho_{eg}(t_0)] - 4ie^{-i\varphi}\Gamma\Omega_R\bar{\Omega} \} \right. \\ & - \sinh\left[\frac{\bar{\Omega}}{4}(t-t_0)\right] (\Gamma(8\Omega_R^2 + \Gamma^2)[\rho_{ge}(t_0) - e^{-2i\varphi}\rho_{eg}(t_0)] - 4ie^{-i\varphi}\Omega_R\{16[\rho_{gg}(t_0) - \rho_{ee}(t_0)]\Omega_R^2 \\ & \left. - [\rho_{gg}(t_0) + 5\rho_{ee}(t_0)]\Gamma^2\} - e^{\frac{1}{4}\Gamma(t-t_0)}\bar{\Omega}(8\Omega_R^2 + \Gamma^2)[\rho_{ge}(t_0) + e^{-2i\varphi}\rho_{eg}(t_0)] + 4ie^{-i\varphi}e^{\frac{3}{4}\Gamma(t-t_0)}\Omega_R\Gamma\bar{\Omega} \} \right\}, \end{aligned} \quad (11)$$

$$\begin{aligned} \rho_{ee}(t) = & \frac{1}{\bar{\Omega}(\Gamma^2 + 8\Omega_R^2)} e^{-\frac{3}{4}\Gamma(t-t_0)} \left\{ -\sinh\left[\frac{\bar{\Omega}}{4}(t-t_0)\right] \{4i\Omega_R(\Gamma^2 + 8\Omega_R^2)[\rho_{eg}(t_0)e^{-i\varphi} - \rho_{ge}(t_0)e^{i\varphi}] \right. \\ & + \Gamma[12\rho_{gg}(t_0)\Omega_R^2 + \rho_{ee}(t_0)(20\Omega_R^2 + \Gamma^2)] \} + \cosh\left[\frac{\bar{\Omega}}{4}(t-t_0)\right] [-4\rho_{gg}(t_0)\Omega_R^2\bar{\Omega} + \rho_{ee}(t_0)\bar{\Omega}(\Gamma^2 + 4\Omega_R^2)] \\ & \left. + 4e^{\frac{3}{4}\Gamma(t-t_0)}\Omega_R^2\bar{\Omega} \right\}, \end{aligned} \quad (12)$$

where  $\rho_{ge} = \rho_{eg}^*$ ,  $\bar{\Omega} \equiv \sqrt{\Gamma^2 - 64\Omega_R^2}$ , and  $\rho_{gg}(t) + \rho_{ee}(t) = 1$ .

The goal of most coherent control procedures is to manipulate the expectation value of some observable of the quantum system, over a given time interval, by means of its coupling with a designed external perturbation. An arbitrary observable of the two-level system can be written in the  $\{|g\rangle, |e\rangle\}$  basis as

$$\mathbf{V} = \begin{pmatrix} v_0 & v \exp(-i\alpha) \\ v \exp(i\alpha) & v_1 \end{pmatrix}, \quad (13)$$

where  $v$ ,  $v_0$ , and  $v_1$  are real values and  $0 \leq \alpha < 2\pi$ . Substituting Eqs. (10)–(13) into Eq. (6) yields

$$\langle \mathbf{V}(t) \rangle = \rho_{gg}(t)v_0 + \rho_{ee}(t)v_1 + 2v \text{Re}[\rho_{ge}(t)\exp(i\alpha)], \quad (14)$$

for the expectation value of  $\mathbf{V}$ , and likewise for the purity of the quantum system,

$$\mathcal{P}(t) = \rho_{gg}^2(t) + \rho_{ee}^2(t) + 2|\rho_{ge}(t)|^2. \quad (15)$$

For the remainder of this study, we apply the quantum-control procedure to manipulate the population of the excited state of the two-level system, therefore  $\mathbf{V} = |e\rangle\langle e|$ , with  $v_1 = 1$

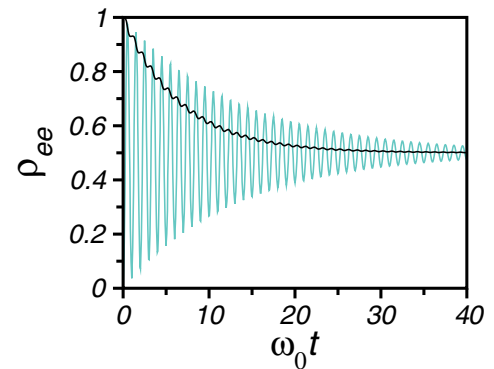


FIG. 1. (Color online) Dynamics of the excited-state population, represented by the reduced density matrix element  $\rho_{ee}(t)$  (blue) and purity  $\mathcal{P}(t)$  of the quantum subsystem (black). The spontaneous decay rate is  $\Gamma = \frac{\omega_0}{5\pi}$ .

and  $v_0 = v = 0$ . Figure 1 shows the damped Rabi oscillations (blue curve) of the excited-state population,  $\rho_{ee}(t)$ , for the two-level system driven by a continuous monochromatic resonant

electromagnetic field and damped by a spontaneous decay rate  $\Gamma = \frac{\omega_0}{5\pi}$ . We define  $\omega_0 = |\mathcal{E}_0|d/2 = \pi$  as the frequency that leads the state of the two-level system over a complete Rabi cycle within a time unit. The purity of the reduced density matrix, given by Eq. (15), is also described in Fig. 1 by the decaying black line. For the chosen decay parameter, the purity of the two-level system vanishes after approximately 10 Rabi cycles.

In the following, we outline the control by reverse optimized pulse sequences. According to this method, a time-dependent external potential produced by the electromagnetic (laser) field is employed to manipulate the quantum dynamics of the two-level system. Thus, the external control parameters are  $\{|\mathcal{E}|, \varphi\}$ , i.e., the intensity and phase of the laser field. As proposed by Kuhn and Luz [30], it is assumed that at determined instants  $t_j$ , the parameters  $\{|\mathcal{E}|, \varphi\}$  of the laser field can be rapidly switched to specified values  $\{|\mathcal{E}_j|, \varphi_j\}$  and then kept constant during the time interval  $\Delta t_{j+1} = t_{j+1} - t_j$ . Such transient time is considered to be much shorter than the characteristic times of the open two-level system. The values  $\{|\mathcal{E}_j|, \varphi_j\}$  are determined *a priori* from instant  $t_j$  so as to satisfy imposed constraints at  $t_{j+1}$ . Thus, within each  $\Delta t_{j+1}$ , the two-level system evolves under the influence of a rectangular electromagnetic pulse characterized by the parameters  $\{|\mathcal{E}_j|, \varphi_j\}$ . The adopted control constraints consist of guiding  $\langle \mathbf{V}(t) \rangle$  along an arbitrary reference trajectory  $S(t)$ , while keeping the purity of the reduced density matrix at its maximum possible value through the instants  $t_j$ . Thus, the parameters  $\{|\mathcal{E}_j|, \varphi_j\}$  are determined in order to minimize the functional  $h[\rho_S(t)]$  at ensuing  $t = t_{j+1}$ ; that is,

$$\{|\mathcal{E}_j|, \varphi_j\} \leftarrow \min(h[\rho_S(t)])|_{t=t_{j+1}}, \quad (16)$$

where

$$h[\rho_S(t)] \equiv \alpha |\langle \mathbf{V}(t) \rangle - S(t)|^2 - \beta \mathcal{P}(t) - \eta (|\mathcal{E}_{j+1}| - |\mathcal{E}_j|)^2. \quad (17)$$

Additional terms can be added to the functional  $h[\rho_S(t)]$ . For instance, the last term on the right side of Eq. (17) is meant to smooth the transition between succeeding pulses. The weights  $\alpha$ ,  $\beta$ , and  $\eta$  can be set arbitrarily to change the relative influence of each component of  $h[\rho_S(t)]$ . For  $\alpha = \beta = \eta = 1$ , the lowest possible value for  $h[\rho_S(t)]$  is  $-1$ . The minimization procedure is carried numerically by the nonlinear conjugate gradient method [35].

#### IV. RESULTS AND DISCUSSION

For an isolated quantum system, or in the limit of vanishing decay rate  $\Gamma \rightarrow 0$ , it is in principle possible to arbitrarily control the quantum dynamics of the two-level system by a sequence of reverse optimized pulses, for instance, by making the excited-state population  $\rho_{ee}(t)$  follow a desired excitation curve, as shown in Fig. 2. In this case, a series of  $N_p = 200$  pulses characterized by the optimized  $\{|\mathcal{E}_j|, \varphi_j\}$  parameters were applied to take the population of the two-level system from the ground state to the excited state. The accordance between the reference curve  $S(t)$  and the time-dependent expectation value  $\langle \mathbf{V}(t) \rangle$  improves as the intervals  $\Delta t_j$  become shorter. A similar quality of control is also obtained for very small decay rate,  $\Gamma < \frac{\omega_0}{50\pi}$ .

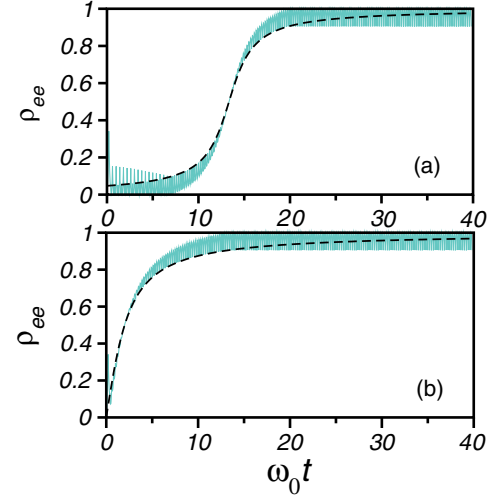


FIG. 2. (Color online) Coherent quantum-control dynamics of the excited-state population  $\rho_{ee}(t)$  (blue) and the reference curve  $S(t)$  (black dashed line) for a closed quantum system ( $\Gamma = 0$ ). A series of  $N_p = 200$  pulses was applied to drive the population inversion. The reference curves are (a)  $S(t) = [\pi/2 + \arctan(t - t')]/\pi$  and (b)  $S(t) = 2 \arctan(t)/\pi$ .

Next we apply the same procedure taking into account the coupling of the quantum subsystem with a Markovian environment via the decay rate  $\Gamma = \frac{\omega_0}{5\pi}$ ; the results are shown in Fig. 3. The reference curve  $S(t) = [\pi/2 + \arctan(t - t')]/\pi$  [same as in Fig. 2(a)] was employed (black dashed curve). The time-dependent population in the excited state,  $\rho_{ee}(t)$ , is described by the blue curve, together with the purity  $\mathcal{P}(t)$  of the quantum subsystem that is represented by a black solid curve. By means of a systematic analysis, the effectiveness of the method was tested for an increasing number of pulse interventions,  $N_p =$  (a) 50, (b) 100, (c) 200, and (d) 300, showing that the control capability of the method improves with the frequency of external pulses, but the target state is never attained. For  $N_p = 50$ , which corresponds to the frequency of pulse interventions  $f_p = 12.5\Gamma$ , there is actually no control upon the two-level system dynamics and even  $\mathcal{P}$  decays faster than at free evolution (Fig. 1). The control efficiency improves for  $N_p = 100$  ( $f_p = 25\Gamma$ ), as shown in Fig. 3(b), and the purity of the subsystem is preserved for some time until the rise of the excited-state population. However, the target state is never attained. If the frequency of the optimized pulse sequence is improved further, for  $f_p = 50\Gamma$  [Fig. 3(c)] or  $f_p = 75\Gamma$  [Fig. 3(d)], then the control performance as well as the purity conservation improve only until the rise of the reference curve, quickly decaying toward an incoherent state afterward. Therefore, the quantum subsystem equilibrates with the environment before the population inversion is completed, irrespective of the rate of external control.

For the problem at hand, we can perform the following analysis assuming that the environment is described by an ohmic bath with a cutoff frequency  $w_c$ . The two-level model approximation is valid if the bandwidth of the electromagnetic pulses ( $\Delta w_p$ ) is not much larger than the characteristic frequency of the system ( $w_0$ ), otherwise off-resonant quantum levels would be coupled by the pulse. Therefore, one can



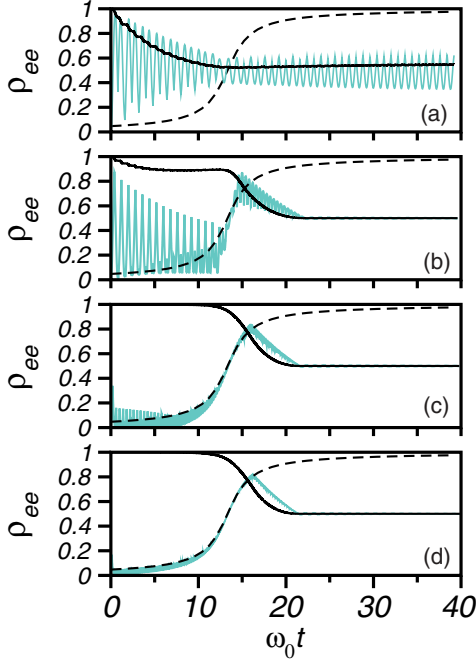


FIG. 3. (Color online) Quantum control of the excited-state population  $\rho_{ee}(t)$  (blue) through the reference curve  $S(t) = [\pi/2 + \arctan(t-t')]/\pi$  (black dashed line) for the quantum subsystem interacting with the environment by  $\Gamma = \frac{\omega_0}{5\pi}$ . Solid (black) line represents the purity  $\mathcal{P}(t)$ . The panels present dynamics due to sequences of an increasing number of pulses:  $f_p =$  (a)  $12.5\Gamma$ , (b)  $25\Gamma$ , (c)  $50\Gamma$ , and (d)  $75\Gamma$ .

qualitatively assume that  $\Delta w_p \simeq w_0$ . For the piecewise quantum-control method, the time duration of the rectangular pulses is approximately  $\Delta t_p = 1/f_p$ , and, furthermore, by invoking the time-frequency uncertainty relation for the pulse [34], we have  $\Delta t_p \Delta w_p \gtrsim \frac{1}{2}$ . Thus, for the slowest train of pulses previously considered ( $N_p = 50$ ), one obtains  $\Delta t_p = 1.25/w_0$  and the ensuing relation  $\Delta w_p \gtrsim 1/(2\Delta t_p) = 0.4w_0$ , which is well within the Markovian condition  $\Delta w_p < w_0 \ll w_c$ . For the fastest train of pulses ( $N_p = 300$ ), which is generally considered to be the condition for improved control efficiency, the same procedure yields  $\Delta w_p \gtrsim 1/(2\Delta t_p) = 2.5w_0$ . In the latter case, the Markovian picture for coherent control of the two-level system becomes problematic and it should be a concern for any practical application of coherent control by pulse sequences. It is important to recall that the characteristic memory time for an ohmic bath is  $\tau \simeq \pi/w_c$  [18].

The same kind of behavior is obtained even if one attempts different population inversion dynamics, for instance by trying to invert the population at once, using the reference curve  $S(t) = 2 \arctan(t)/\pi$ , as shown in Fig. 4. The overall behavior is similar to the previous case, as shown in Fig. 3. The collapse of the coherent control is caused by the competition between the buildup of quantum coherences, which is induced by the electromagnetic pulses, and the dissipation process. If the system starts from the ground state, midway along the increasing reference curve, the quantum system is found in a state with  $\rho_{ee} = \rho_{gg} = 1/2$  and  $|\rho_{ge}| \lesssim 1/2$ . By examining Eqs. (9a), and setting  $\rho_{ee} = \rho_{gg} = 1/2$ , one finds that  $\dot{\rho}_{ge} \sim$

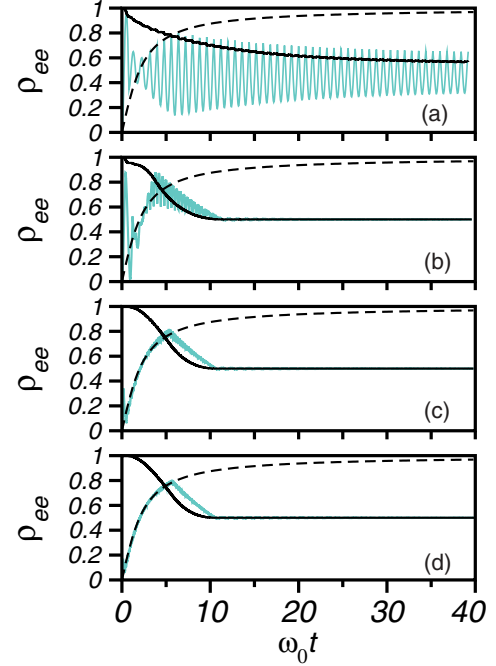


FIG. 4. (Color online) Quantum control of the excited-state population  $\rho_{ee}(t)$  (blue) through the reference curve  $S(t) = 2 \arctan(t)/\pi$  (black dashed line) for the quantum subsystem interacting with the environment by  $\Gamma = \frac{\omega_0}{5\pi}$ . Solid (black) line represents the purity  $\mathcal{P}(t)$ . The panels present dynamics due to sequences of an increasing number of pulses:  $f_p =$  (a)  $12.5\Gamma$ , (b)  $25\Gamma$ , (c)  $50\Gamma$ , and (d)  $75\Gamma$ .

$-\gamma_{eg}\rho_{ge}$ , which is the strongest dissipation regime. As the train of pulses continues to push  $\rho_{ee} \rightarrow 1$  and  $|\rho_{ge}| \rightarrow 1/2$ , an overshoot of dissipation occurs and the system ends up in the statistical mixture.

Figure 5 shows the behavior of the system ( $\rho_{ee}$  and  $\mathcal{P}$  represented by blue and black curves, respectively) for a reference curve that is a decreasing function of time (dashed

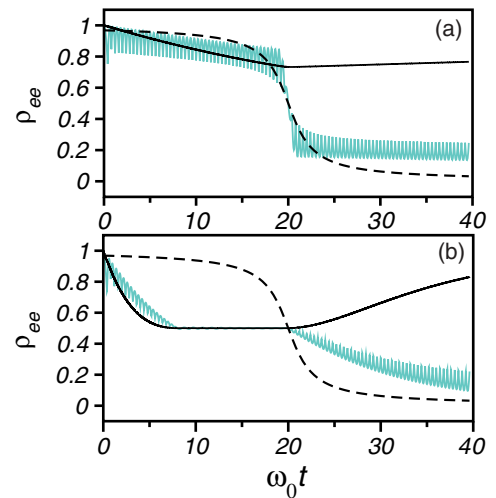


FIG. 5. (Color online) Quantum control of the excited-state population  $\rho_{ee}$  (blue line) through a decaying reference curve  $S(t)$  (black dashed line) The decay constant is (a)  $\Gamma = \frac{\omega_0}{50\pi}$  and (b)  $\Gamma = \frac{\omega_0}{5\pi}$ . Solid black line represents the purity  $\mathcal{P}(t)$ . The frequency of the pulse sequence is  $f_p = 25\Gamma$  for (a) and (b).

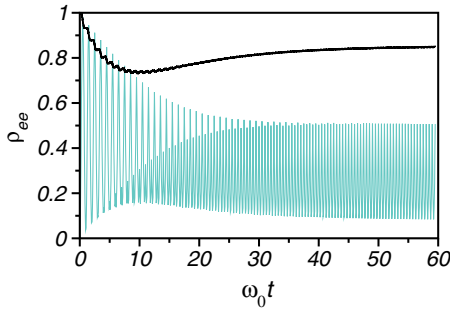


FIG. 6. (Color online) Dynamical decoupling of the quantum subsystem:  $\rho_{ee}(t)$  is described by the blue curve and  $\mathcal{P}$  in the black curve,  $\Gamma = \frac{\omega_0}{5\pi}$ , and  $\omega_p = 2\omega_0$ .

curve). For a small decay parameter  $\Gamma = \frac{w_0}{50\pi}$  [see Fig. 5(a)], the excited-state population follows the reference curve and the coherent control is attained. For  $\Gamma = \frac{w_0}{5\pi}$  [see Fig. 5(b)],  $\rho_{ee}$  does not follow the reference curve and, moreover, the purity decays faster than in the unperturbed case. The spontaneous decay from unstable quantum systems can be suppressed, under restricted conditions, by sufficiently frequent measurements in the quantum Zeno (QZ) framework. Analogous effects have also been studied for a sequence of unitary pulses [7,8,29,37,38] considering structured reservoirs or within the strong-coupling limit between system and environment. It is important to emphasize, though, that the acceleration of the decay process (anti-QZ effect) is more ubiquitous than the suppression case [39]. Our simulations for a two-level system coupled to a Markovian environment in the moderate dissipation regime,  $\Gamma = w_0/(5\pi)$ , exhibit the anti-QZ behavior. In Fig. 5(b), as the reference curve decays toward zero, it dumps the quantum system in the ground state, decoupling it from the environment and increasing  $\mathcal{P}$  as a consequence.

By changing the guiding curve  $S(t)$  to a step function, one can momentarily accomplish a population inversion, but decoherence quickly destroys the quantum control. So far we have used the set of weights  $\alpha = \beta = \eta = 1$  in Eq. (17) to obtain the previous results; nevertheless, the behavior is qualitatively the same for different weight distributions.

The previous analysis indicates that active coherent quantum-control schemes based on a train of pulses can only work effectively for closed quantum systems or an open quantum system with a small decay constant, in our case  $\Gamma < \frac{\omega_0}{50\pi}$ . Nevertheless, a train of pulses with a high-repetition rate can be used to decouple the quantum two-level system from the environment, preserving its purity at high values over time, as shown in Fig. 6. In this case, after an initial transient decay, the pulses partially recover the purity and keep  $\mathcal{P} \approx 0.85$  in the steady state, above the value  $\mathcal{P} = 0.5$  for the incoherent statistical mixture. The decoupling effect is observed, irrespective of the initial conditions, only for  $f_p = \frac{w_0}{\pi}$ , wherein the reverse optimization algorithm yields a sequence of pulses with phase differences,  $|\varphi_{j+1} - \varphi_j| = \pi$ . The decoupling effect has been extensively discussed in the literature in the context of spin relaxation and quantum optics [7,8,29,36,38].

In Secs. II and III, the quantum master equation was derived assuming the Markovian regime and the weak-coupling limit

between the quantum system and the environment. Under such conditions, it has been shown that active coherent control by pulse sequences cannot overcome the dissipative quantum dynamics because in Markovian open systems the environment irreversibly dissipates the quantum system information. However, for a slow reservoir with a narrow spectral width, in the non-Markovian limit, quantum control can still be possible for some time interval, since the non-Markovian features of the bath help to maintain the coherences in the quantum subsystem. Non-Markovian systems are common in all branches of physics, including quantum optics and condensed-matter physics. In biological systems, for instance, the distinct protein-solvent interactions are considered to be responsible for the quantum coherences observed in the light-harvesting centers of natural photosynthetic units [32,40]. The development of femtosecond pulse shaping has made it possible to induce Rabi oscillations in single molecules at room temperature over a time of a few hundred femtoseconds [41].

## V. CONCLUSIONS

We have extended the method of active quantum control via reverse optimized pulse sequences [30] by taking into account decoherence and dissipation effects produced by the coupling with a Markovian environment. The effectiveness of the quantum-control procedure is investigated under dissipative dynamics conditions for a model quantum two-level system. The quantum Liouville equation was used, in the Lindblad form, to describe the quantum subsystem weakly coupled with a Markovian environment. The reverse design of the pulses was performed through the minimization of the functional  $h[\rho_S(t)]$ , given by Eq. (17), by means of a nonlinear conjugate gradient method. The adopted control criterion consisted of guiding the mean value of an observable of the quantum subsystem along a reference trajectory,  $S(t)$ , while keeping the purity of the reduced density matrix at its maximum. Although the method performs well for pure quantum systems, the dissipative quantum dynamics hinders its accomplishment for moderate decay constants, even for high-repetition pulse sequences or steplike guiding curves. For the assumed Markovian bath, the effectiveness of the method is recovered for small decay rates,  $\Gamma < \frac{\omega_0}{50\pi}$ . The collapse of the coherent control is ascribed to a dissipation overshoot that happens midway through the population inversion, even for a train of short pulses. In addition, attempts to suppress the spontaneous decay from the metastable excited state showed the prevalence of the anti-Zeno behavior for moderate dissipation rates,  $\Gamma = \frac{\omega_0}{5\pi}$ . However, if the metastable two-level system is long lived and only phase decoherence affects its short-term dynamics, then the external quantum control could be improved. The method is suited, nonetheless, for dynamical decoupling of the quantum subsystem from the environment, in which case the purity can be maintained at high values by a sequence of  $\pi$  pulses.

## ACKNOWLEDGMENTS

Financial support for this work was provided by the Brazilian funding agencies CNPq and CAPES.

- [1] *Information Complexity and Control in Quantum Physics*, edited by A. Blaquiére, S. Diner, and G. Lochak (Springer, New York, 1987).
- [2] A. Butkovskiy and Y. Samoilenko, *Control of Quantum-Mechanical Process and Systems* (Kluwer, Boston, 1990).
- [3] H. Ezawa and Y. Murayama, *Quantum Control and Measurement* (North-Holland, New York, 1993).
- [4] H. Rabitz, R. de Vivie-Riedle, M. Motzkus, and K. Kompa, *Science* **288**, 824 (2000).
- [5] S. Rice and M. Zhao, *Optical Control Of Molecular Dynamics* (Wiley, New York, 2000).
- [6] R. Gordon and S. Rice, *Annu. Rev. Phys. Chem.* **48**, 601 (1997).
- [7] L. G. C. Rego, L. F. Santos, and V. S. Batista, *Annu. Rev. Phys. Chem.* **60**, 293 (2009).
- [8] R. Saha and V. S. Batista, *J. Phys. Chem. B* **115**, 5234 (2011).
- [9] A. P. Peirce, M. A. Dahleh, and H. Rabitz, *Phys. Rev. A* **37**, 4950 (1988).
- [10] R. Kosloff, S. Rice, O. Gaspard, S. Tersigni, and D. Tannor, *Chem. Phys.* **139**, 201 (1989).
- [11] M. Shapiro and P. Brumer, *J. Chem. Phys.* **84**, 4103 (1986).
- [12] R. S. Judson and H. Rabitz, *Phys. Rev. Lett.* **68**, 1500 (1992).
- [13] J. Geremia, W. Zhu, and H. Rabitz, *J. Chem. Phys.* **113**, 10841 (2000).
- [14] G. Huang, T. Tarn, and J. Clark, *J. Math. Phys.* **24**, 2608 (1983).
- [15] M. Dahleh, A. P. Peirce, and H. Rabitz, *Phys. Rev. A* **42**, 1065 (1990); W. Warren, H. Rabitz, and M. Dahleh, *Science* **259**, 1581 (1993); V. Ramakrishna *et al.*, *ibid.* **51**, 960 (1995).
- [16] *Decoherence: Theoretical, Experimental, and Conceptual Problems*, edited by P. Blanchard, D. Giulini, E. Joos, C. Kiefer, and I. Stamatescu (Springer, New York, 2000).
- [17] D. Braun, *Dissipative Quantum Chaos and Decoherence* (Springer, New York, 2001).
- [18] A. Nitzan, *Chemical Dynamics in Chemical Phases: Relaxation, Transfer and Reactions in Condensed Molecular Systems* (Oxford University Press, New York, 2006).
- [19] N. Doslic, K. Sundermann, L. Gonzalez, O. Mo, J. Giraud-Girard, and O. Kuhn, *Phys. Chem. Chem. Phys.* **1**, 1249 (1999).
- [20] Y. Ohtsuki, K. Nakagami, Y. Fujimura, W. Zhu, and H. Rabitz, *J. Chem. Phys.* **114**, 8867 (2001).
- [21] W. Zhu and H. Rabitz, *J. Chem. Phys.* **118**, 6751 (2003).
- [22] P. W. Shor, *Phys. Rev. A* **52**, R2493 (1995).
- [23] A. M. Steane, *Phys. Rev. Lett* **77**, 793 (1996).
- [24] E. Knill and R. Laflamme, *Phys. Rev. A* **55**, 900 (1997).
- [25] E. Knill, *Nature (London)* **434**, 39 (2005).
- [26] P. Aliferis, D. Gottesman, and J. Preskill, *Quantum Inf. Comput.* **6**, 97 (2006).
- [27] K. Khodjasteh and D. A. Lidar, *Phys. Rev. Lett.* **95**, 180501 (2005); *Phys. Rev. A* **75**, 062310 (2007).
- [28] G. S. Uhrig, *Phys. Rev. Lett.* **98**, 100504 (2007); W. Yang and R.-B. Liu, *ibid.* **101**, 180403 (2008).
- [29] L. Viola and S. Lloyd, *Phys. Rev. A* **58**, 2733 (1998); *Phys. Rev. Lett.* **82**, 2417 (1999).
- [30] J. Kuhn and M. G. E. da Luz, *Phys. Rev. A* **75**, 053410 (2007).
- [31] H.-P. Breuer and F. Petruccione, *The Theory of Open Quantum Systems* (Oxford University Press, New York, 2002).
- [32] J. Eckel, J. H. Reina, and M. Thorwart, *New J. Phys.* **11**, 085001 (2009).
- [33] P. Lambropoulos and D. Petroyan, *Fundamentals of Quantum Optics and Quantum Information* (Springer-Verlag, Berlin Heidelberg, 2007).
- [34] C. Rullière, *Femtosecond Laser Pulses* (Springer-Verlag, Berlin Heidelberg, 2005).
- [35] J. R. Shewchuk, *An Introduction to the Conjugate Gradient Method Without the Agonizing Pain*, Technical Report, Carnegie Mellon University, Pittsburgh, PA, 1994 (unpublished).
- [36] P. Facchi, D. A. Lidar, and S. Pascazio, *Phys. Rev. A* **69**, 032314 (2004).
- [37] L. Viola and E. Knill, *Phys. Rev. Lett.* **94**, 060502 (2005).
- [38] G. S. Agarwal, M. O. Scully, and H. Walther, *Phys. Rev. Lett.* **86**, 4271 (2001).
- [39] A. G. Kofman and G. Kurizki, *Nature (London)* **405**, 546 (2000); A. G. Kofman, G. Kurizki, and T. Opatrny, *Phys. Rev. A* **63**, 042108 (2001).
- [40] G. S. Engel, T. R. Calhoun, E. L. Read, T. K. Ahn, T. Mancal, Y. C. Cheng, R. E. Blankenship, and G. R. Fleming, *Nature (London)* **446**, 782 (2007).
- [41] R. Hildner, D. Brinks, and N. F. van Hulst, *Nature Phys.* **7**, 172 (2011).